PHOTOCATALYTIC DEGRADATION OF RhB OVER GRAPHENE-BASED Ag/AgBr COMPOSITES

XINYUAN KANG, ZHIPING WU, FANG LIAO, TINGTING GUO, SHIZHEN ZHAO and XUN SONG

Chemical Synthesis and Pollution Control
      Key Laboratory of Sichuan Province
School of Chemistry and Chemical Industry
China West Normal University
Nanchong 637002
P. R. China
e-mail: liaozhang2003@163.com

Abstract

In this paper, a simple hydrothermal method was developed for the preparation of micro-nanocomposite rGO/Ag/AgBr using ascorbic acid as a reducing agent. It could completely decompose $5 \, mg \, L^{-1}$ RhB under 250W UV light irradiation within 160 min. The catalytic activity was discovered to be strongly affected by the some operating parameters, such as solution pH, catalytic amount, and graphene doping amount. The possible photocatalytic mechanism of the rGO/Ag/AgBr composite was also discussed. Our results indicated that rGO nanosheets played a role of a highly efficient cocatalyst for the rapid transfer of photo generated electrons. rGO/Ag/AgBr photocatalysts exhibited highly efficient and stable photo degradation for RhB under UV irradiation.

1. Introduction

Currently, as a kind of photocatalysts, silver/silver halide (Ag/AgX, X = Cl, Br) has been widely used in photo degradation of the pollutants [1-8], because silver/silver halide has a small band gap [1, 6]. Actually, Ag/AgBr displays higher catalytic activity than Ag/AgCl because Br^0 has a lower electron affinity than Cl^0 [6]. However, the aggregation of the Ag/AgBr particles is still severe. In recent years, much attention has been paid to grapheme (rGO) because of its compelling physical properties and various applications [9-13]. Graphene is a robust two-dimensional sheet of sp^2-hybridized carbon. Especially, a great development has been achieved as a support for catalysts because of its high surface area and special electronic transport properties [10-12]. However, researchers seldom pay attention to the graphene-based photocatalytic materials, because of the severe aggregation of rGO [11, 13] and poor water solubility [14]. Graphene oxide (GO), a graphene sheet functionalized with oxygen groups, provides fertile opportunities for the construction of GO-based hybrid composites on account of its good solubility in solvents [15]. Based on the above considerations, it is very necessary to develop and prepare the novel rGO/Ag/AgX. Meanwhile, Ag/AgX particles can be dispersed well on the graphene surface in order to avoid accumulation.

As known, the synthesis method is very important to develop highly efficient silver halide photocatalysts. Nowadays, Ag@AgCl/RGO hybrids has been prepared [16]. $AgBr/Ag/Ag_2O/GO$ composite has also been fabricated [17]. Ag/AgBr/rGO has also been synthesized via a facile solution-mixing method [18]. However, in our work, a simple one-pot route is developed for preparing graphene-based Ag/AgBr composites in the hydrothermal reaction. It is also used to degrade RhB to test the catalytic capacity under ultraviolet light (UV) irradiation. We further discussed photocatalytic efficiency in different solution pH, catalytic amount, graphene doping amount, and the possible photocatalytic mechanism of the rGO/Ag/AgBr composites. It is believed that this strategy can be extended to fabricate other rGO-semiconductors composites in the future.

2. Experiment

2.1. Materials

Ultra pure water was used and its resistivity was > 18 MΩ cm. $AgNO_3$, hexadecyltrimethyl ammonium bromide (CTAB) and ascorbic acid were purchased from Cheng du Ke Long. All chemicals were of analytical grade and used without further purification.

2.2. Preparation of rGO/Ag/AgBr

GO was synthesized by a modified Hummers method [19]. Figure 1 showed a schematic illustration of ther GO/Ag/Ag Br synthesis process. Typical synthetic process of rGO/Ag/AgBr nanocomposite was as follows: 0.01g GO was dissolved into 15mL deionized water. Then, 0.2g hexadecyltrimethyl ammonium bromide (CTAB), 0.20385g $AgNO_3$, and 0.352g ascorbic acid were added into the above GO aqueous solution. After being mixed uniformly, the mixture was poured into a 50ml Teflon-lined stainless steel autoclave, which was sealed and heated at 160°C for 12h. After cooling to room temperature, the product was collected by centrifugation, washed with water/ethanol several times, and dried in a vacuum oven at 60ºC for 24h. Thereinto, CTAB can not only provide Br^- to obtain AgBr but serve as a surfactant. What's more, GO was reduced by ascorbic acid.
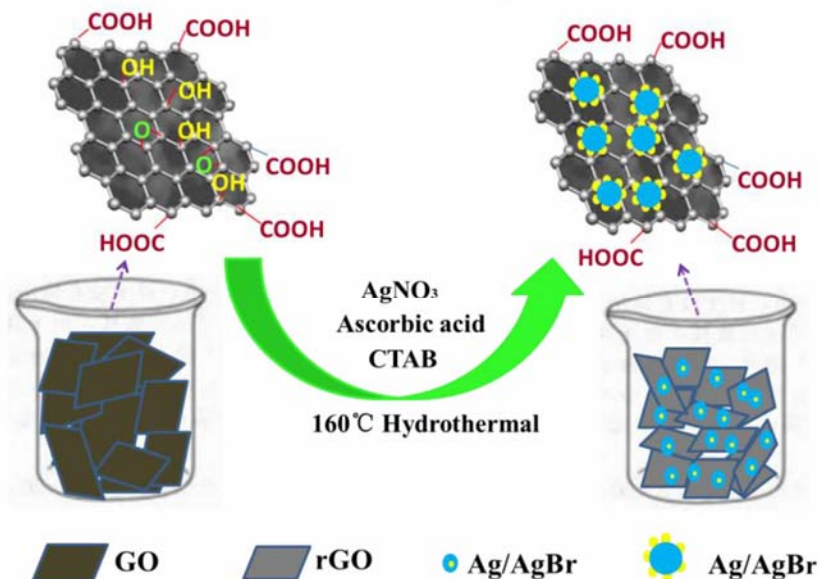
Figure 1. A schematic illustration of the synthesis process of rGO/Ag/AgBr.

3. Results and Discussion

3.1. Characterization of rGO/Ag/AgBr

rGO/Ag/AgBr was characterized by the typical scanning electron microscopy (SEM) (Figure 2(a), (b)) and transmission electron microscopy (TEM) (Figure 2(c), (d)) from the low-magnification image to the high-magnification image, respectively. As shown in Figure 2(a), (b), many micro-nano spheres were prepared with the diameter of about 800nm, which were uniformly embedded on the graphene. Thereinto, the rGO sheets could be observed clearly in the rGO/Ag/AgBr hybrids (Figure 2(a)) and (Figure 2(c), (d)). What's more, Ag/AgBr particles were seen on the basal planes of the grapheme (Figure 2(c), (d)).
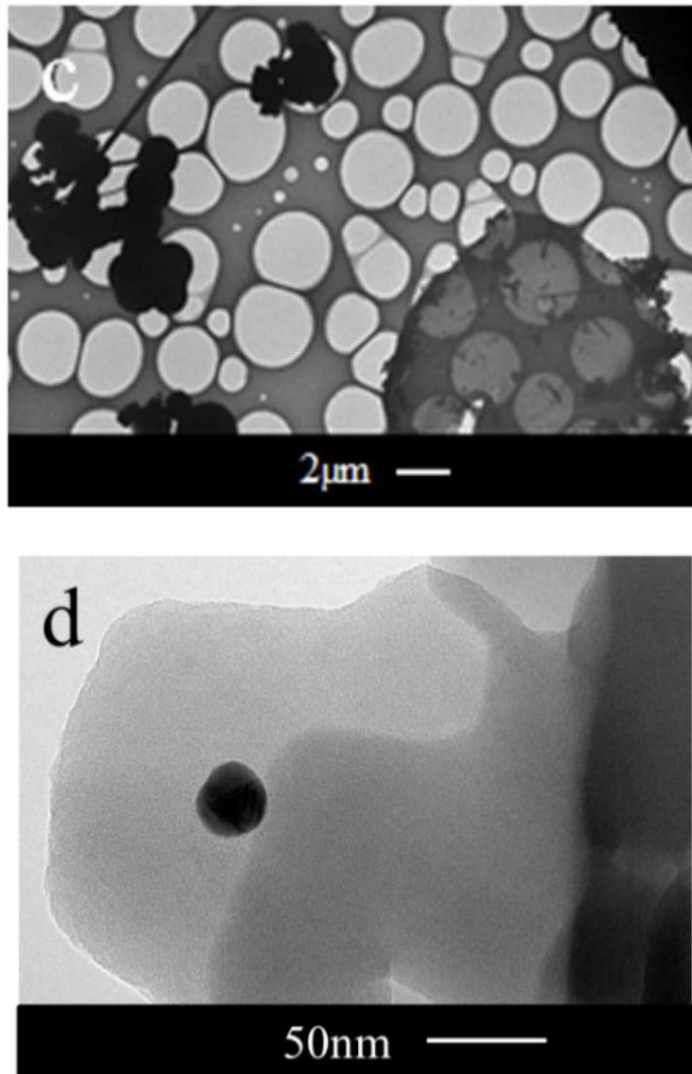
10μm
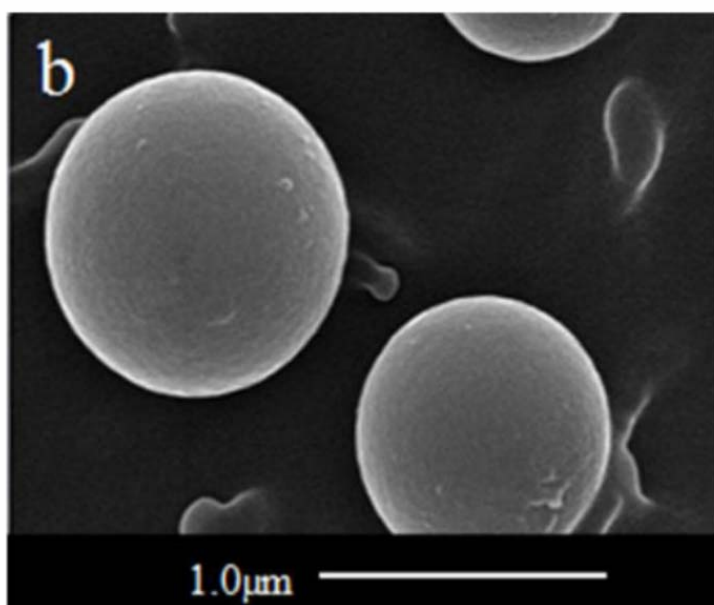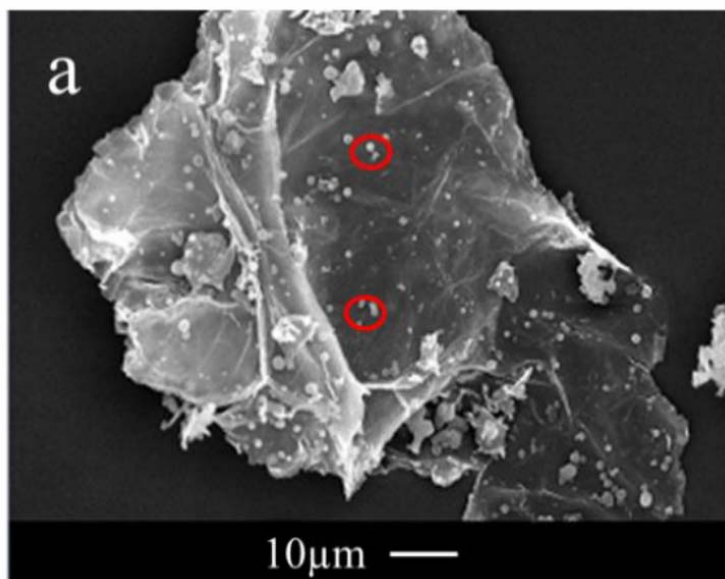
Figure 2. rGO/Ag/AgBr SEM picture of (a) low magnification, (b) high magnification, and TEM diagram of (c) low magnification, (d) high magnification.

The chemical composition of the hybrids was determined by energy-dispersed spectrum (EDS) (Figure 3(a)). The C peak may come from the presence of graphene. The peak of Ag and Br element may be attributed to AgNPs and AgBr. To further confirm the phase structure, the typical XRD pattern was shown in Figure 3(b). All diffraction peaks could be specified as two group's peaks, " " of Ag and " " of AgBr. The XRD pattern of rGO/Ag/AgBr displayed distinct diffraction peaks (2θ) at 26.7°(111), 30.9°(200), 44.3°(220), 55.0°(222), 64.5°(400), 73.2°(420) and 38.2°(111), 44.3°(200), 64.5°(220), 77.4°(311), which were due to the diffractions of cubic phase of AgBr (JCPDS file: 06-0438) and that of metallic Ag (JCPDS file: 04-0783), respectively. What's more, no diffraction peak for the synthetic rGO was observed in the composite. It may be caused by the low amount (1.3%) relatively and low diffraction intensity of graphene [20].
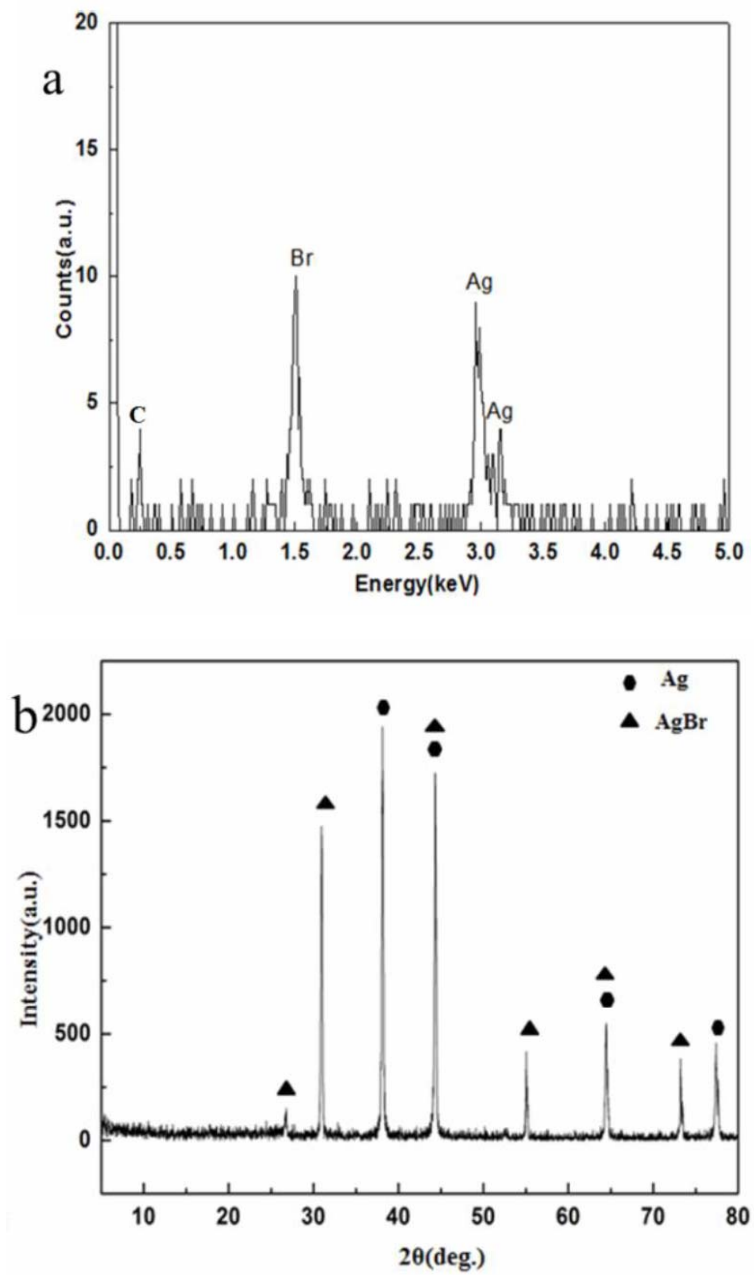
Figure 3. The EDS spectrum (a) and the XRD patterns (b) of rGO/Ag/AgBr.

3.2. Catalytic activity of rGO/Ag/AgBr

A photo degradation experiment of RhB was executed to test photocatalytic efficiency of rGO/Ag/AgBr composites under UV irradiation at room temperature. On the basis of the Beer_Lambert law, the concentration of RhB was linearly proportional to the intensity of the absorption peak at 553nm. Consequently, the decomposition efficiency of RhB can be calculated by using the following calculation formula:

$$\text{RhB decomposition (\%)} = \frac{C_0 - C_n}{C_0} \times 100\%,$$

thereinto, C_0 and C_n were defined as the equilibrium concentrations of RhB before and after UV irradiation, respectively. The UV light was provided by a 250W ultraviolet lamp. The concentration of RhB dye was determined by a ultraviolet-visible (UV/Vis) spectrophotometer. As shown in Figure 4, the photo degradation time of RhB was 30 min in the dark for the as-manufactured rGO/Ag/AgBr and Ag/AgBr. It was so fast because RhB molecules and rGO-based hybrids produced the intermolecular $\pi - \pi$ interactions [20, 21]. As shown the blank experiment in Figure 4, it was negligible for the self-photosensitized decomposition of RhB. However, it was up to 97.9% to degradate RhB for rGO/Ag/AgBr as a photocatalyst, but only about 2.4% and 36% in terms of the blank and Ag/AgBr composite during the same 160 min UV irradiation. The results indicated that the photocatalytic activity of the rGO/Ag/AgBr could obviously increase for RhB degradation by hybridizing with rGO nano sheets. This may be attributed to the smaller size and the reinforced charge transfer in terms of rGO/Ag/AgBr [2]. In addition, the enhanced degradation efficiency of RhB can be clearly proved by the change of the UV-vis absorption spectra of the solution (Figure 4(b)). It was found that two changes happened in the absorption spectra of the solution with the increase of irradiation time. Maximum absorption peak rapidly reduced, meanwhile the wavelength blue-shift happened. The wavelength blue shift indicated that higher energy was needed for the electron transition and the demethylated RhB molecule had been formed in the process of degradation [22-24].
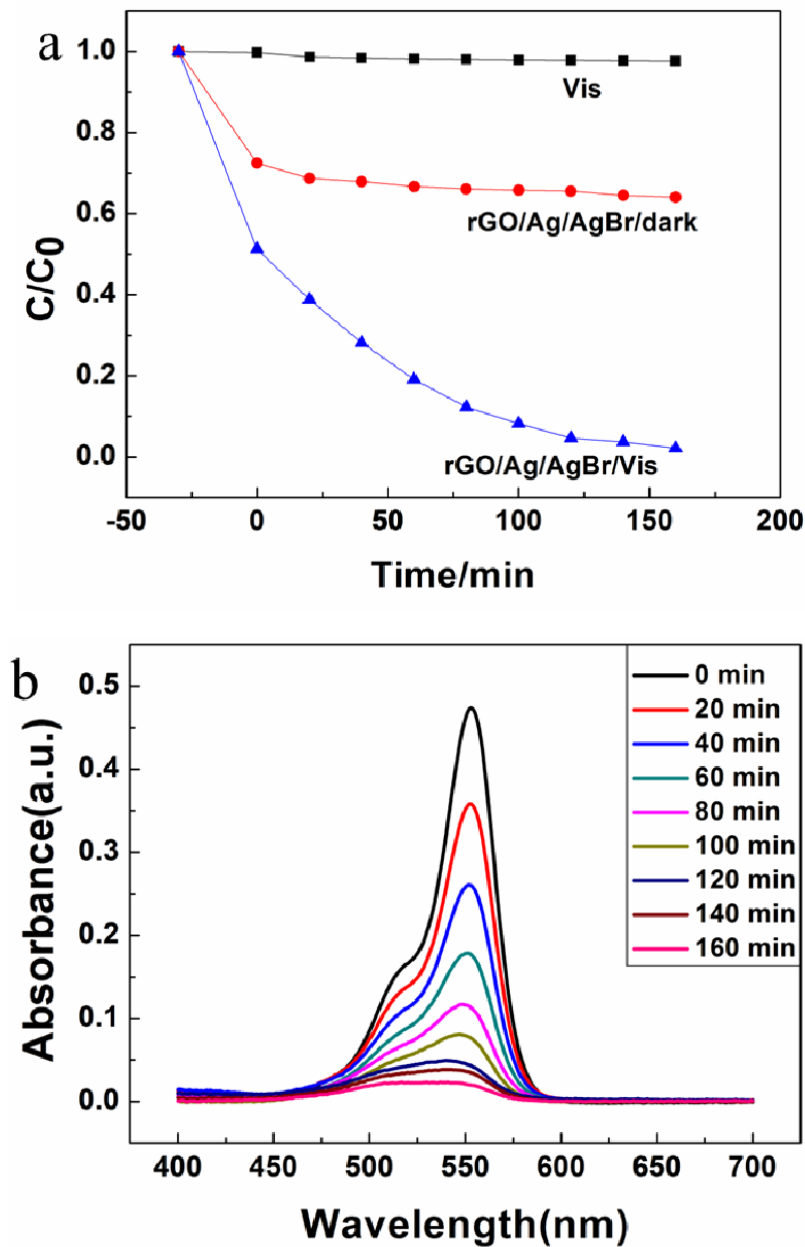
Figure 4. (a) Degradation of RhB under different conditions. (b) The UV-vis spectral changes of RhB. Experimental conditions: RhB, 40mL, $5mgL^{-1}$; rGO/Ag/AgBr, 0.015g (1.3 wt% rGO); and initial pH = 6.

As known, the solution pH was an important factor in catalytic reaction. The rGO/Ag/AgBr catalyst could work effectively over a wide pH range from 2.0 to 9.0 in Figure 5. Obviously, the degradation rate of RhB gradually increased with pH from 2.0 to 6.0 but then sharply decreased at pH 9. This could be attributed to the fact that AgBr fractionated out a few Ag^+, which converted to Ag_2O in alkaline environment [25]. As a consequence, rGO/Ag/AgBr was not stable in alkaline medium. And the degradation efficiency of rGO/Ag/AgBr was weakened. The RhB solution of pH 6 was chosen as the supporting condition for the further work. The effect of rGO/Ag/AgBr amount was investigated under given reaction condition. As shown in Figure 6, the adsorption ability and the photocatalytic efficiency for RhB accordingly increased with catalyst amount from 0.005g to 0.015g. However, when the catalyst dosage was increased to 0.02g, the degradation efficiency was not further enhanced but decreased. It may be attributed to the opacity of rGO/Ag/AgBr, which prevented the Ag/AgBr from absorbing UV-visible light. Then, it led to the combination of electron-hole pairs in rGO/Ag/AgBr and reduced the photocatalytic efficiency of RhB [26, 27]. Consequently, suitable catalyst content was crucial for optimizing the photocatalytic performance. In order to investigate the role of graphene in photocatalytic process, different amount of graphene doped rGO/Ag/AgBr was also detected. As shown in Figure 7, the photocatalytic activity for RhB accordingly increased with graphene loading from 0 wt% to 1.3 wt%. As a electronic conductor, rGO effectively reinforced charge transfer and suppressed combination of electron-hole pairs in rGO/Ag/AgBr [11, 12]. What's more, a hydrophobic graphene with bigger specific surface area improved the adsorption sites of organic molecules RhB [11]. However, when graphene loading reached up to 2.6%, a drastic decrease was observed in the photocatalytic activity. This may be also due to the increase of the opacity by high grapheme loading, which prevented AgBr from absorbing UV-visible light [26, 27]. For this reason, 1.3% graphene loading was chosen as the supporting condition for the whole work.
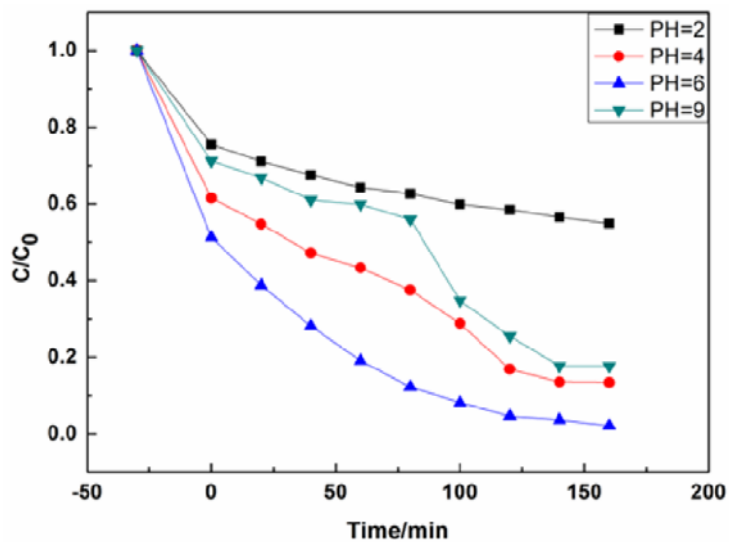
Figure 5. Effect of initial PH on the degradation of RhB over rGO/Ag/AgBr/UV light system. Experimental conditions: RhB, 40mL, 5mgL^{-1}; rGO/Ag/AgBr, 0.015g (1.3 wt% rGO).

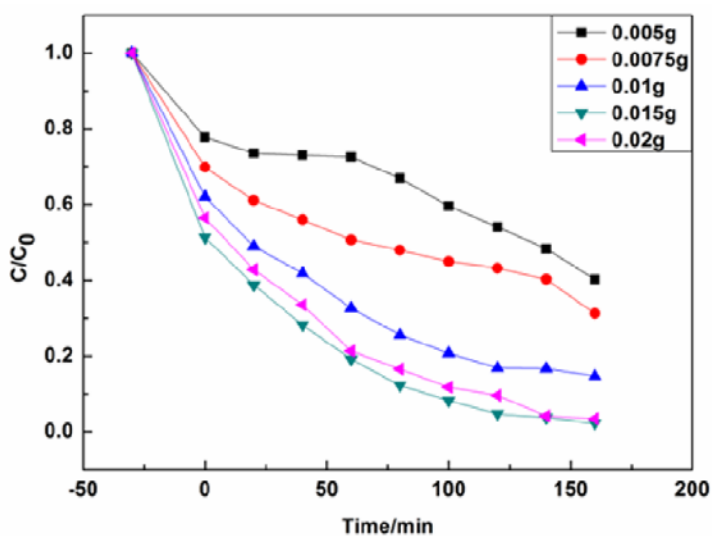**Figure 6.** Effect of catalyst amount on the degradation of RhB over rGO/Ag/AgBr/UV light system. Experimental conditions: RhB, 40mL, 5mgL^{-1}; rGO/Ag/AgBr, 0.015g (1.3 wt% rGO); and initial pH = 6.

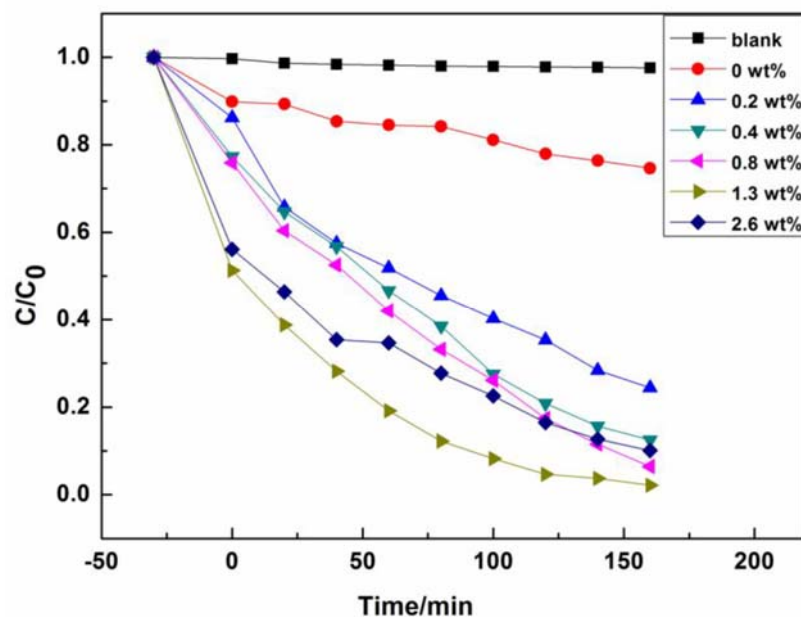**Figure 7.** Effect of graphene amount on the degradation of RhB over rGO/Ag/AgBr/UV light system. Experimental conditions: RhB, 40mL, 5mgL^{-1}; rGO/Ag/AgBr, 0.015g (0, 0.2, 0.4, 0.8, 1.3, 2.6 wt% rGO); and initial pH=6.

As seen from Figure 8, GCE, Ag/AgBr, and rGO/Ag/AgBr were investigated about AC impedance spectra in 0.01mol/L $K_3[Fe(CN)_6] / K_4[Fe(CN)_6]$. From the AC impedance spectra, the radius size of the capacitive arc represented the electron transfer resistance. Obviously, the smaller the radius size of the capacitive arc was, the smaller the electrode surface electron transfer resistance was. Compared with GCE and Ag/AgBr, rGO/Ag/AgBr can make electron transfer faster on electrode surface. Therefore, the rGO nanosheets played a role of a highly efficient co catalyst for rapidly transferring photo generated electrons. Figure 9 indicated the degradation efficiency of rGO/Ag/AgBr for RhB. In our work, the rGO/Ag/AgBr photocatalyst was handled by centrifugation each time and was reused for three times. As shown in

Figure 9, only a slight decrease could be seen in terms of the photocatalytic activity. It may be caused by light corrosion or dissolution of the rGO/Ag/AgBr photocatalyst. Obviously, rGO/Ag/AgBr composites exhibited high efficiency and better stability on the decolorization of RhB under UV irradiation. Compared with other photocatalysts such as α-Fe_2O_3 microspheres [28] and BiOBr-Ag [29], rGO/Ag/AgBr also showed better photocatalytic activity.
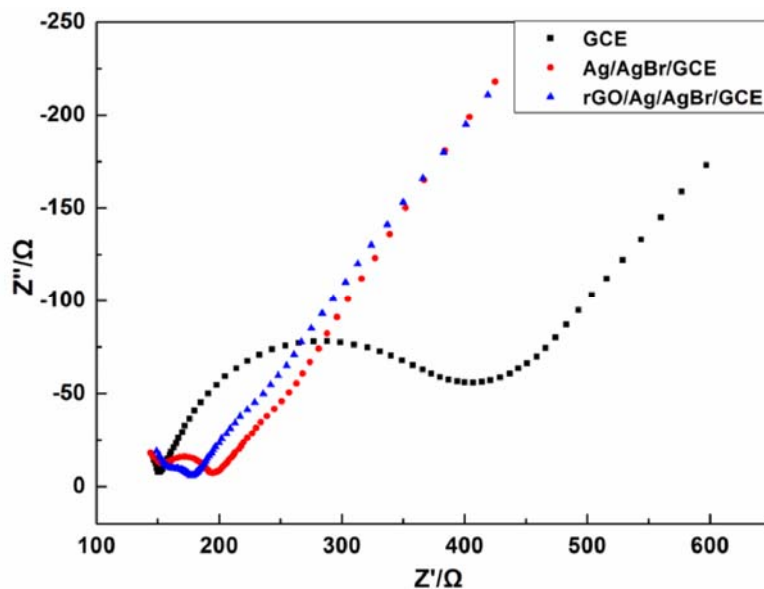

Figure 8. Comparison of Nyquist plots of GCE, Ag/AgBr and rGO/Ag/AgBr.
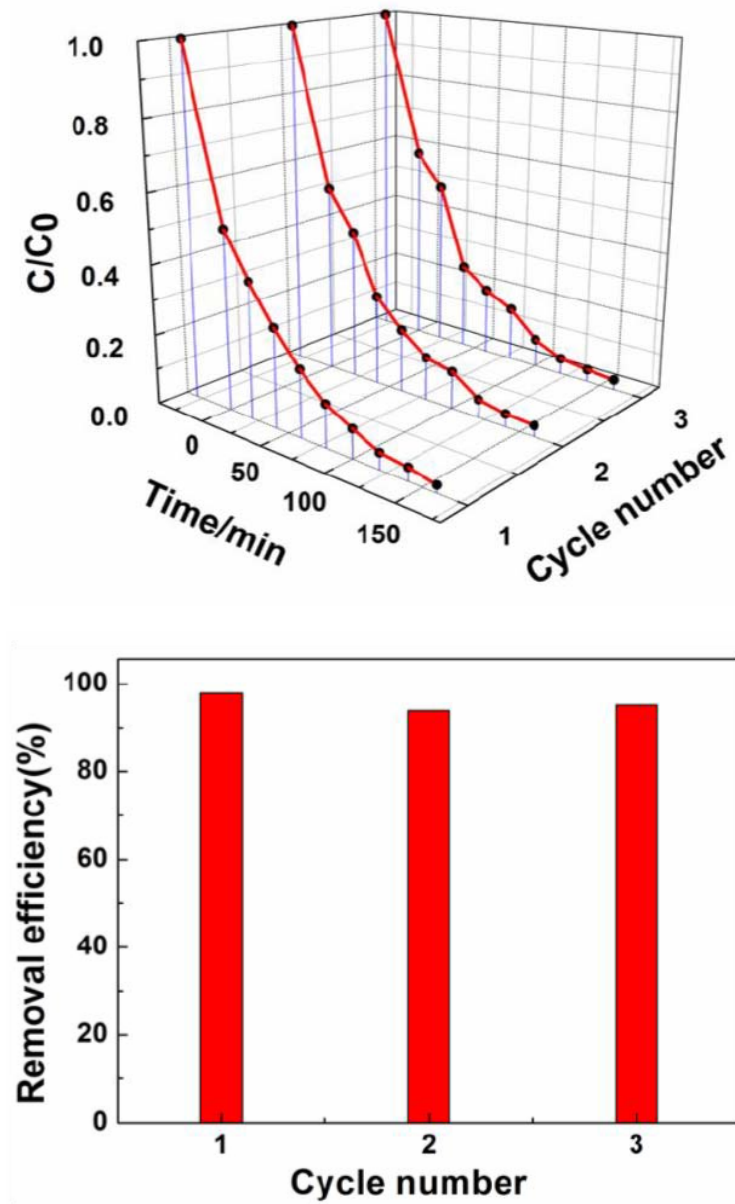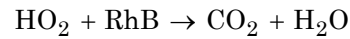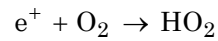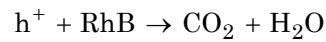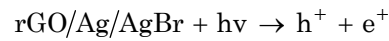
Figure 9. Cycling kinetic curves (a) and cyclability (b) over rGO/Ag/AgBr/UV light system. Experimental conditions: RhB, 40mL, 5mgL^{-1}; rGO/Ag/AgBr, 0.015g (0.8 wt% rGO); and initial pH = 6.

The possible photocatalytic mechanism of the rGO/Ag/AgBr composites were also discussed in Figure 10. The photocatalytic degradation of organic substances occurred on the surface of the photocatalyst [30]. In our work, RhB molecules on the surface of rGO/Ag/AgBr photocatalyst were adsorbed on the rGO via $\pi - \pi$ conjugation [20]. AgBr could not absorb UV light because of its wide band gap. However, metallic AgNPs can generate photo generated electrons and transfer to AgBr under UV light. Then the photo generated electrons can be effectively transferred from AgBr to rGO surface by the strong interaction. Thus, electrons on the surface of the graphene reduced oxygen to obtain HO_2, while the photo generated holes (h^+) were retained on the surface of AgNPs to oxidize organic RhB molecule [8, 31, 32]. In this process, the rGO nanosheets played a role of a highly efficient cocatalyst to rapidly transfer photo generated electrons. These processes resulted in a lower recombination rate and enhanced photocatalytic activity [26].
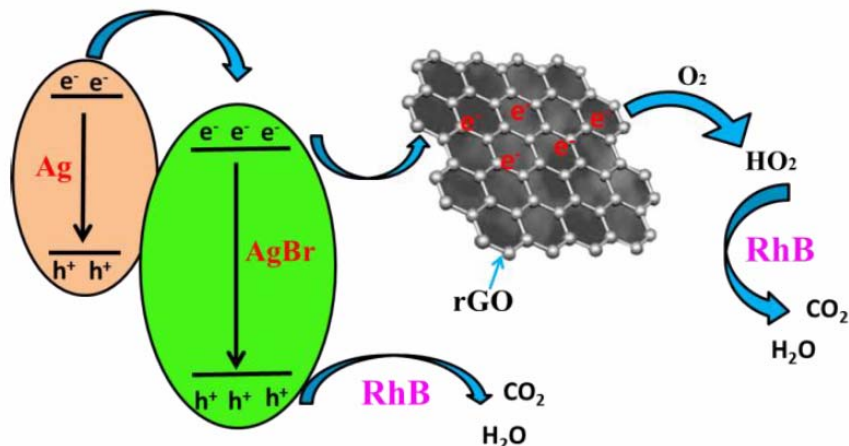
$$rGO/Ag/AgBr + hv \rightarrow h^+ + e^+$$

$$h^+ + RhB \rightarrow CO_2 + H_2O$$

$$e^+ + O_2 \rightarrow HO_2$$

$$HO_2 + RhB \rightarrow CO_2 + H_2O$$

Figure 10. Schematic diagram of electron-hole pairs separation and the possible reaction mechanism over rGO/AgBr/Ag hybrid photocatalyst under UV light irradiation.

4. Conclusion

In summary, the UV-driven rGO/Ag/AgBr photocatalyst was successfully prepared by a facile hydrothermal method. Compared with Ag/AgBr, as-manufactured rGO/Ag/AgBr had better UV-driven photocatalytic activity under the same experimental conditions. The products were not only applied for polluted water disposal fields but provided promising applications in photo degradation and other fields, such as sensors, biomedical engineering, and magnetics.

Acknowledgement

References

[1]   M. S. Zhu, P. L. Chen and M. H. Liu, Langmuir 28 (2012), 3385-3390.

[2]   M. S. Zhu, P. L. Chen and M. H. Liu, ACS Nano 5 (2011), 4529-4536.

[3]   C. H. An, S. Peng and Y. G. Sun, Adv. Mater. 22 (2010), 2570-2574.

[4]   Y. Y. Li and Y. Ding, J. Phys. Chem. C 114 (2010), 3175-3179.

[5]   L. Kuai, B. Y. Geng, X. T. Chen, Y. Y. Zhao and Y. C. Luo, Langmuir 26 (2010), 18723-18727.

[6]   P. Wang, B. Huang, X. Zhang, X. Qin, H. Jin, Y. Dai, Z. Wang, J. Wei, J. Zhan, S. Wang, J. Wang and M. H. Whangbo, Chem. Eur. J. 15 (2009), 1821-1824.

[7]   X. F. Wang, S. F. Li, Y. Q. Ma, H. G. Yu and J. G. Yu, J. Phys. Chem. C 115 (2011), 14648-14655.

[8]   G. Q. Luo, X. J. Jiang, M. J. Li, Q. Shen, L. M. Zhang and H. G. Yu, ACS Appl. Mater. Interfaces 5 (2013), 2161-2168.

[9]   H. Chen, S. X. Zhou and L. M. Wu, ACS Appl. Mater. Interfaces 6 (2014), 8621-8630.

[10] S. Y. Toh, K. S. Loh, S. K. Kamarudin and W. R. Wan Daud, Chem. Eur. J. 251 (2014), 422-434.

[11] M. S. A. S. Shah, A. R. Park, K. Zhang, J. H. Park and P. J. Yoo, ACS Appl. Mater. Interfaces 4 (2012), 3893-3901.

[12] P. N. Zhu, A. S. Nair, S. J. Peng, S. Y. Yang and S. Ramakrishna, ACS Appl. Mater. Interfaces 4 (2012), 581-585.

[13] T. N. Lambert, C. A. Chavez, B. Hernandez-Sanchez, P. Lu, N. S. Bell, A. Ambrosini, T. Friedman, T. J. Boyle, D. R. Wheeler and D. L. Huber, J. Phys. Chem. C 113 (2009), 19812-19823.

[14] Y. Gao, X. Pu, D. Zhang, G. Ding, X. Shao and J. Ma, Carbon 50 (2012), 4093-4101.

[15] A. Lerf, H. He, M. Forster and J. Klinowski, J. Phys. Chem. B 102 (1998), 4477-4482.

[16] Zhang, X. F. Fan, X. Quan, S. Chen and H. T. Yu, Environ. Sci. Technol. 45 (2011), 5731-5736.

[17] J. S. Xie, L. S. Li, Y. C. Guan, H. D. Lu, C. L. Han, D. F. Zhao, C. G. Tian and Q. Y. Yin, Materials Letters 120 (2014), 54-57.

[18] X. H. Meng, X. S. H. Y. Li, J. Yin, J. Wang, F. Z. Liu, X. H. Liu, M. Wang and H. L. Zhong, Materials Letters 105 (2013), 162-165.

[19] William S. Hummers Jr. and Richard E. Offeman, J. Am. Chem. Soc. 80 (1958), 1339-1339.

[20] H. Zhang, X. J. Lv, Y. M. Li, Y. Wang and J. H. Li, ACS Nano 4 (2010), 380-386.

[21]   S. D. Perera, R. G. Mariano, K. Vu, N. Nour, O. Seitz, Y. Chabal and K. J. Balkus, ACS Catal. 2 (2012), 949-956.

[22]   Z. H. Ai, L. R. Lu, J. P. Li, L. Z. Zhang, J. R. Qiu and M. H. Wu, J. Phys. Chem. C 111 (2007), 4087-4093.

[23]   Z. H. Ai, L. R. Lu, J. P. Li, L. Z. Zhang, J. R. Qiu and M. H. Wu, Phys. Chem. C 111 (2007), 7430-7436.

[24]   C. C. Chen, X. Z. Li, W. H. Ma and J. C. Zhao, J. Phys. Chem. B 106 (2002), 318-324.

[25]   Y. Xu and F. M. Jiang, The Study on Synthesis of Silver Bromide Nanoparticles and its Photocatalytic Activity (Master Dissertation from Jilin University in 2011).

[26]   W. G. Wang, J. G. Yu, Q. J. Xiang and B. Cheng, Appl. Catal. B-Environ. 119(120) (2012), 109-116.

[27]   S. W. Liu, C. Liu, W. G. Wang, B. Cheng and J. G. Yu, Nanoscale 4 (2012), 3193-3200.

[28]   T. T. Zhang, T. T. Guo, Z. P. Wu, S. W. Yang, Z. F. Wang and F. Liao, NANO: Brief Reports and Reviews 8 (2013), 1350053(1)-1350053(7).

[29]   Q. Q. Fang, Y. J. You and C. H. Li, Guangzhou Chemical Industry 42 (2014), 100-102.

[30]   Y. H. Zhang, Z. R. Tang, X. Z. Fu and Y. J. Xu, ACS Nano 4 (2010), 7303-7314.

[31]   X. F. Wang, S. F. Li, Y. Q. Ma, H. G. Yu and J. G. Yu, J. Phys. Chem. C 115 (2011), 14648-14655.

[32]   X. Wang, S. Li, H. Yu, J. Yu and S. Liu, Chem. Eur. J. 17 (2011), 7777-7780.

■